J Appl Electrochem (2014) 44:1–4
DOI 10.1007/s10800-013-0617-3

SHORT COMMUNICATION

Photoelectrochemical properties of Fe-doped TiO_2 nanotube arrays fabricated by anodization

Xixin Wang · Jianling Zhao · Yingru Kang · Lanlan Li · Xingru Xu

Received: 4 May 2013 / Accepted: 18 August 2013 / Published online: 24 August 2013

Abstract Ti–Fe alloys with Fe contents of 0.05, 0.5 and 1.0 wt% were obtained using the arc-melting method. Fe-doped TiO_2 nanotube arrays were prepared by anodizing Ti–Fe alloys in ethylene glycol solution containing 0.25 wt% NH_4F and 10 wt% H_2O. The microstructure, crystal structure and photoelectrochemical properties of the nanotube arrays were characterized using scanning electron microscopy, X-ray diffraction, UV–Vis diffuse reflectance spectroscopy and electrochemical analyzer. Results show that doping of 0.05 wt% Fe improves the photoelectrochemical properties of titania nanotube arrays significantly, whilst further increasing the Fe contents to 0.5 and 1.0 wt% degrades these properties. The external potential has a considerable influence on the photocurrent density at doping content of 0.5 wt% Fe.

Keywords Titania nanotube · Fe doping · Photoelectrochemical property · Anodization

1 Introduction

The fabrication of titania nanotube arrays by anodization method has been studied extensively over the past decade due to their unique structure and excellent properties [1–3]. The photoelectrochemical properties of nanotube arrays are strongly enhanced compared to a compact film since the titania nanotubes are vertically aligned on a conducting substrate, which restrains the recombination of photogenerated electrons and photogenerated holes and increases the rate of electron transfer [4, 5]. The wide bandgap of TiO_2, however, limits its activation to UV radiation [6, 7]. In order to shift the bandgap of TiO_2, various surface modification methods including deposition of metal or semiconductor onto the surface of titania nanotube arrays have been investigated [8, 9]. An alternative modification method involves introducing doping elements into the crystal structure of titania nanotube arrays [10, 11]. One effective method is to first prepare Ti alloy containing the target doping element and then anodize the Ti alloy to obtain the modified titania nanotube arrays [12, 13]. Apparent modification effects have been reported on the anodization of Ti–Pd, Ti–V, Ti–W alloy, etc. [14–16].

It is well known that doping with the right amount of Fe improves the photoelectrochemical activity of titania effectively [17–20]. Even some work has been reported on the preparation of Fe-doped nanotube arrays through anodizing of Ti–Fe alloy [21]; very little is known about the influences of Fe content on the photoelectrochemical properties. In this paper, different contents of Fe were introduced into titanium by using the alloying method, and Fe-doped titania nanotube arrays were achieved by anodization. Photoelectrochemical properties of the Fe-doped and undoped titania nanotube arrays have been studied for comparative analysis. The influence of Fe content on the photoelectrochemical properties has also been discussed.

2 Experimental procedures

Titanium and Ti–Fe alloy (containing 0.05 wt% Fe, 0.5 wt% Fe and 1 wt% Fe) were prepared by mixing titanium and iron powders (99.9 % purity) in proportion and melting in an arc-melting furnace under an argon atmosphere. The smelted samples were cut into 10 × 10 × 0.5 mm^3 foils using a

X. Wang · J. Zhao (✉) · Y. Kang · L. Li · X. Xu
School of Material Science and Engineering, Hebei University of Technology, Tianjin 300130, China
e-mail: zhaojl02@126.com

linear cutting machine. They were polished with metallographic abrasive paper and ultrasonically washed in twice-distilled water and acetone prior to use. Anodization was carried out using a program-controlled DC source (Dahua Coop., Beijing, China). The anodization setup consisted of two-electrode configuration with titanium or Ti–Fe alloy foil as anodic electrode and platinum foil ($10 \times 20 \times 0.1$ mm^3) as the cathodic electrode. The distance between anodic and cathodic electrodes was 20 mm. Electrolytes in this process were ethylene glycol solution containing 0.25 wt% NH_4F and 10 wt% H_2O. All solutions were prepared from analysis grade chemicals and deionized water. All anodization experiments were conducted at room temperature at 60 V for 8 h. During the experiments, the solutions were stirred with a magnetic stirrer. After anodization, the samples were rinsed in deionized water, air dried and characterized.

After anodization, the samples were annealed at 460 °C in air for 4 h before further measurements. UV–Vis diffuse reflectance spectra were recorded using a Cary 300 UV–Vis–NIR spectrometer (Varian, USA). The photocurrent density was measured using LK2005 electrochemical analyzer (Lanlika, China). The photoresponse under irradiation was measured in a standard three-electrode configuration composed of a sample as working electrode, a platinum foil as counter electrode and a saturated calomel electrode (SCE) as a reference electrode, 0.5 M Na_2SO_4 as the electrolyte. The working electrode was irradiated from a UV lamp (8 W, main wavelength 254 nm) or a high pressure mercury lamp (250 W, main wavelength 365, 410 and 440 nm).

3 Results and discussion

Surface and cross-sectional SEM images of the undoped and Fe-doped titania nanotube arrays are shown in Fig. 1. Surface morphologies of the undoped and doped samples were similar (Fig. 1a, b) and the nanotubes compactly arranged with a length of about 6.5 μm from the cross-sectional view inserted in Fig. 1a, b.

Figure 2 gives the X-ray diffraction patterns of undoped and 0.5 wt% Fe-doped samples after annealing at 460 °C for 4 h. XRD results indicate that the annealed samples for undoped and Fe-doped titania nanotube arrays were of anatase crystals (pdf Card No. 21-1272). The titanium peaks come from the substrate due to the porous structure of the thin films.

The photoelectrochemical properties were studied when the annealed samples were irradiated from a UV lamp (8 W) or a high pressure mercury lamp (250 W), respectively. The curves of photocurrent density versus external potential in the range of 0.0–1.0 V are shown in Figs. 3 and 4. As illustrated in Fig. 3, under UV lamp irradiation, when doping content of Fe is 0.05 wt%, the photocurrent density is obviously higher than the other samples and the photocurrent density decreases with increasing Fe content. The photocurrent density of the sample containing 0.5 wt% Fe is similar to that of the undoped sample (Fig. 3a, c), and when doping content of Fe is 1.0 wt%, its photocurrent density is lower than that of undoped sample (Fig. 3a, d). As illustrated in Fig. 4, under irradiation of high pressure mercury lamp, the photocurrent density of the sample containing 0.05 wt% Fe is similar to that of the sample containing 0.5 wt% Fe (Fig. 4b, c), and both samples have a higher photocurrent density than that of undoped titania nanotube arrays. The photocurrent is minimum for the sample containing 1.0 wt% Fe.

In Figs. 3 and 4, the relative value of photocurrent density of the 0.05 wt% Fe-doped sample, undoped sample and 1.0 wt% Fe-doped sample is similar, the order is: 0.05 wt% Fe-doped sample > undoped sample > 1.0 wt% Fe-doped sample. As for the 0.5 wt% Fe-doped sample, under UV lamp irradiation, its photocurrent density is similar to that of the undoped sample (Fig. 3a, c), whilst under irradiation with a high pressure mercury lamp, its photocurrent density is similar to that of 0.05 wt% Fe-doped sample (Fig. 4b, c). Photocurrent density of all the samples increases with increasing external potential (Figs. 3 and 4). Under irradiation of high pressure mercury lamp, the photocurrent density of 0.5 wt% Fe-doped sample changes more noticeably with the external potential than that of other samples (Fig. 4).

Fe^{3+} and Ti^{4+} have similar radius and different ion valence states. Compared with undoped titania, the Fe-doped samples have more oxygen vacancies and defects. These defects act as electron capturers and produce more free carriers under light irradiation. In addition, these defects might also act as the carrier recombination centers and hinder the production of free carrier [18, 20]. At lower doping content (0.05 wt% Fe), there are fewer defects in the sample, to act as electron capturers, improve the separation efficiency and prolong the lifetime of photoinduced carriers, and increase the photocurrent density accordingly. At higher doping content (1.0 wt% Fe), there are excess defects in the sample, the photoinduced electrons are bound to the acceptor level of Fe and act as recombination centers. Recombination probability of photoinduced electrons and holes increases and the photoinduced current density decreases. At moderate doping content (0.5 wt% Fe), the sample's inner defects have similar effects on the separation and recombination of electrons and holes, and the photocurrent is close to the undoped sample.

The UV–Vis absorption spectra of undoped and 0.5 wt% Fe-doped sample are shown in Fig. 5. Compared with the undoped sample, the band edge of 0.5 wt% Fe-doped sample moved to longer wavelength and the

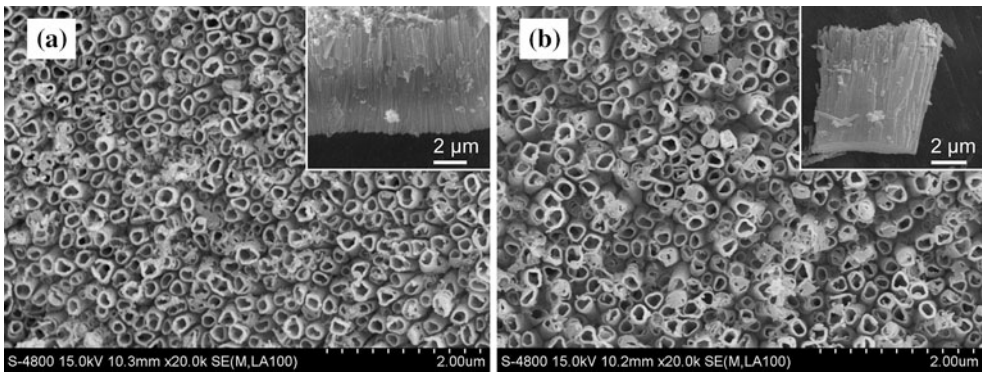

Fig. 1 Surface and cross-sectional SEM images of undoped (**a**) and 0.5 wt% Fe-doped titania nanotube arrays (**b**)

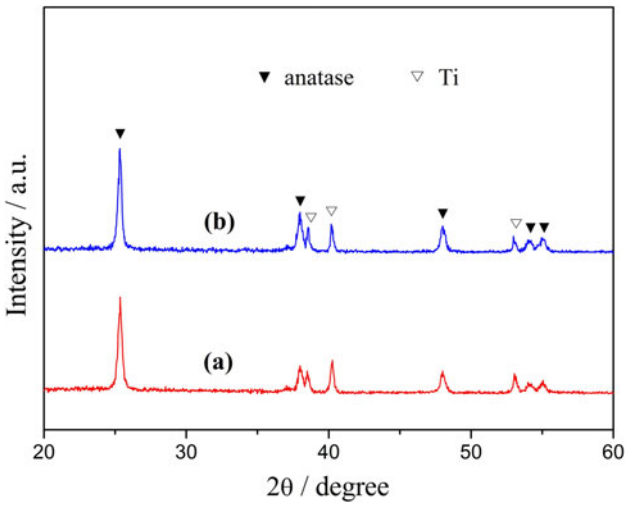

Fig. 2 XRD patterns of annealed samples *a* undoped titania nanotube arrays, *b* 0.5 wt% Fe-doped titania nanotube arrays

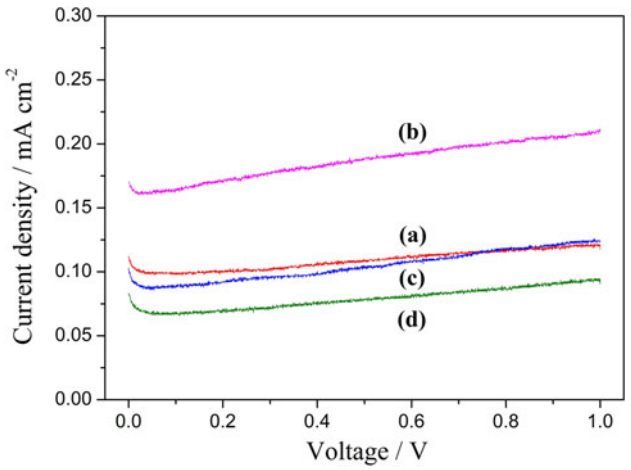

Fig. 3 Photocurrent response of the undoped (*a*) and Fe-doped (*b* 0.05 wt% Fe, *c* 0.5 wt% Fe, *d* 1.0 wt% Fe) samples under irradiation of UV lamp

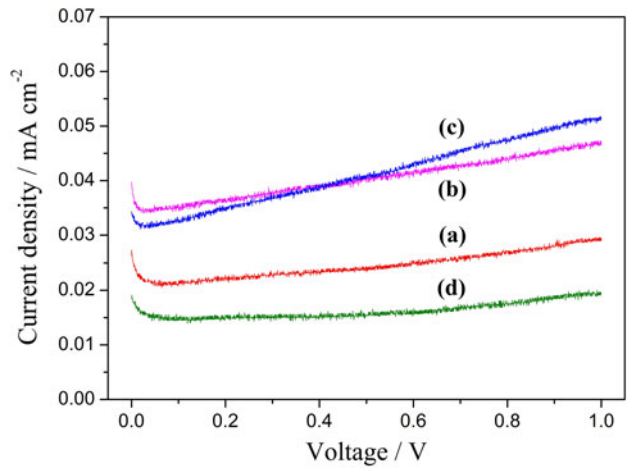

Fig. 4 Photocurrent response of the undoped (*a*) and Fe-doped (*b* 0.05 wt% Fe, *c* 0.5 wt% Fe, *d* 1.0 wt% Fe) samples under irradiation of high-pressure mercury lamp

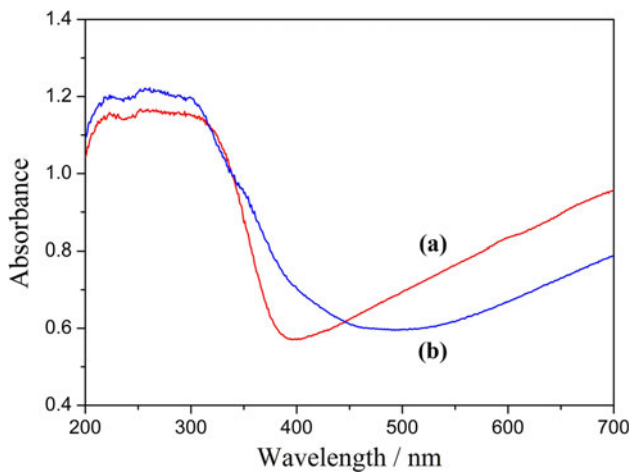

Fig. 5 UV–Vis absorption spectra of undoped (*a*) and 0.5 wt% Fe doped (*b*) titania nanotube arrays

UV–Visible absorption band reached 460 nm. For the 0.5 wt% Fe-doped sample, the photocurrent density increase under irradiation of high pressure mercury lamp can be attributed to the redshift of adsorption edge. The external potential has more noticeable influence on the separation of electrons and holes when the doping content

is moderate and the photocurrent density would increase significantly with the external potential (Fig. 4c).

4 Conclusions

Fe-doped titania nanotube arrays were prepared by anodizing the Ti–Fe alloys, and anatase nanotube arrays were obtained after annealing the samples at 460 °C. Doping of 0.05 wt% Fe can obviously improve photoelectrochemical property of titania nanotube arrays, and further increasing the contents of Fe would decrease their property. The photocurrent density increases with increasing external potential. At moderate doping content (0.5 wt% Fe), the defects have similar effects on the separation and recombination of electrons and holes, and the external potential has a greater influence on the photocurrent density.

Acknowledgments This work is supported by National Natural Science Foundation of China (No. 51272064), Key Basic Research Program of Hebei Province of China (No. 12965135D), the Excellent Youth Foundation of Hebei Province Scientific Committee of China (E2013202032) and the Talent Training Project of Hebei Province (2013).

References

1. Chen B, Lu K (2012) Hierarchically branched titania nanotubes with tailored diameters and branch numbers. Langmuir 28(5): 2937–2943
2. Vasilev K, Poh Z, Kant K, Chan J, Michelmore A, Losic D (2010) Tailoring the surface functionalities of titania nanotube arrays. Biomaterials 31(3):532–540
3. Zhao J, Wang X, Chen R, Li L (2005) Fabrication of titanium oxide nanotube arrays by anodic oxidation. Solid State Commun 134(10):705–710
4. John SE, Mohapatra SK, Misra M (2009) Double-wall anodic titania nanotube arrays for water photooxidation. Langmuir 25(14):8240–8247
5. Varghese OK, Paulose M, Grimes CA (2009) Long vertically aligned titania nanotubes on transparent conducting oxide for highly efficient solar cells. Nat Nanotechnol 4(9):592–597
6. Aziz AA, Yong KS, Ibrahim S, Pichiah S (2012) Enhanced magnetic separation and photocatalytic activity of nitrogen doped titania photocatalyst supported on strontium ferrite. J Hazard Mater 199:143–150
7. Antoniadou M, Panagiotopoulou P, Kondarides DI, Lianos P (2012) Photocatalysis and photoelectrocatalysis using nanocrystalline titania alone or combined with Pt, RuO_2 or NiO co-catalysts. J Appl Electrochem 42(9):737–743
8. Liu Y, Zhou H, Zhou B, Li J, Chen H, Wang J, Bai J, Shangguan W, Cai W (2011) Highly stable CdS-modified short TiO_2 nanotube array electrode for efficient visible-light hydrogen generation. Int J Hydrogen Energy 36(1):167–174
9. Sun L, Li J, Wang C, Li S, Lai Y, Chen H, Lin C (2009) Ultrasound aided photochemical synthesis of Ag loaded TiO_2 nanotube arrays to enhance photocatalytic activity. J Hazard Mater 171(1):1045–1050
10. Yoon J, Kim S, No K (2012) Highly ordered and well aligned TiN nanotube arrays fabricated via template-assisted atomic layer deposition. Mater Lett 87:124–126
11. Mohamed AER, Rohani S (2011) Modified TiO_2 nanotube arrays (TNTAs): progressive strategies towards visible light responsive photoanode, a review. Energy Environ Sci 4(4):1065–1086
12. Nah Y-C, Shrestha NK, Kim D, Schmuki P (2013) Electrochemical growth of self-organized TiO_2–WO_3 composite nanotube layers: effects of applied voltage and time. J Appl Electrochem 43(1):9–13
13. Kim D, Tsuchiya H, Fujimoto S, Schmidt-Stein F, Schmuki P (2012) Nitrogen-doped TiO_2 mesosponge layers formed by anodization of nitrogen-containing Ti alloys. J Solid State Electrochem 16(1):89–92
14. Allam NK, Poncheri AJ, El-Sayed MA (2011) Vertically oriented Ti–Pd mixed oxynitride nanotube arrays for enhanced photoelectrochemical water splitting. ACS Nano 5(6):5056–5066
15. Yang Y, Kim D, Schmuki P (2011) Electrochromic properties of anodically grown mixed V_2O_5–TiO_2 nanotubes. Electrochem Commun 13(10):1021–1025
16. Zhao J, Wang X, Kang Y, Xu X, Li Y (2008) Photoelectrochemical activities of W-doped titania nanotube arrays fabricated by anodization. Photonics Technol Lett 20(14):1213–1215
17. Wu Q, Ouyang J, Xie K, Sun L, Wang M, Lin C (2012) Ultrasound-assisted synthesis and visible-light-driven photocatalytic activity of Fe-incorporated TiO_2 nanotube array photocatalysts. J Hazard Mater 199:410–417
18. Pang YL, Abdullah AZ (2012) Effect of low Fe^{3+} doping on characteristics, sonocatalytic activity and reusability of TiO_2 nanotubes catalysts for removal of Rhodamine B from water. J Hazard Mater 235:326–335
19. Sun L, Li J, Wang C, Li S, Chen H, Lin C (2009) An electrochemical strategy of doping Fe^{3+} into TiO_2 nanotube array films for enhancement in photocatalytic activity. Sol Energy Mater Sol Cells 93(10):1875–1880
20. Zhou M, Yu J, Cheng B, Yu H (2005) Preparation and photocatalytic activity of Fe-doped mesoporous titanium dioxide nanocrystalline photocatalysts. Mater Chem Phys 93(1):159–163
21. Li G, Zhang W, Zhang J, Li Y, Kang X, Tang H (2011) A novel way to fabricate Fe doped TiO_2 nanotubes by anodization of Ti–Fe alloys. Rare Metal Mater Eng 40(9):1510–1513